Exploring the full potential of a sparse nodes survey in the Western Gulf of Mexico

Feng Lin, Dorothy Ren, Jiawei Mei, Zhiguang Xue (CGG); Joakim Blanch, Marcus Cahoj, Jon Jarvis, Alex Kostin (BHP)*

Summary

The western part of the Gulf of Mexico (WGOM) is often characterized by large and complex salt and shale bodies, making it notoriously challenging to image deep subsalt targets, especially with only wide-azimuth towed-streamer (WATS) data available. In 2018, BHP acquired a large-scale sparse ocean bottom node (OBN) survey in this region as a cost-effective way to derive a more accurate velocity through full-waveform inversion (FWI) for WATS data imaging. The relatively large shot spacing, compounded by the complex overburden and the strong reliance on long-offset data (>40 km) for deeper model updates, poses considerable challenges to the processing of this sparse nodes survey. We present how we mitigated the noise issue accompanying this sparse nodes survey and how we made better use of the long-offset data to unlock the full potential of this data set, ultimately obtaining both an improved velocity model and improved images in this complex area. We also demonstrate that using a better low-frequency source can increase the S/N of long-offset sparse nodes data and further improve the velocity models updated by FWI.

Introduction

The western part of the Gulf of Mexico is an area of complex geology with large salt and shale bodies that are very challenging for seismic imaging. The area of interest in this study is located at the corners of East Breaks, Garden Banks, Alaminos Canyon, and Keathley Canyon, with water depth of ~2 km. It has subsalt targets at a depth of ~12 km, below thick salt bodies with extremely undulated bases of salt and complex sediment inclusions around the salt bases. Prior to 2018, two sets of WATS data were acquired and processed multiple times with extensive salt scenario work and state-of-the-art technologies, such as tomography using reverse time migration (RTM) 3D angle gathers and FWI, to better image and understand the geology in this region. However, the subsalt images remain very poor for the following reasons: first, the complex salt geometry is not easily resolved by manual interpretation; second, earlier FWI algorithms did not work on salt; and third, the existing WATS data is not sufficient for model building and imaging in this area.

With improvements in the algorithm, FWI has become a powerful tool for automatic velocity model building in salt environments (Shen et al., 2017; Michell et al., 2017; Zhang et al., 2018; Wang et al., 2019). OBN has also proved to be the best data type for FWI in geologically challenging regions given its full azimuth, ultra-long offsets, and good low-frequency signal-to-noise ratio (S/N). Driven primarily by improved FWI algorithms and available OBN data, we have experienced a step-change improvement in subsalt imaging in the last few years (Wang et al., 2019; Nolte et al., 2019). However, OBN has mostly been used for development fields within a small survey area rather than large-scale exploration, mainly due to its high cost. For that reason, Dellinger et al. (2017) propose to acquire sparse OBN data for velocity model building with FWI while using existing streamer data for imaging for large-scale exploration projects, while also demonstrating the feasibility of this idea with synthetic data. Through a decimation study using the dense Atlantis OBN field data, Mei et al. (2019) prove that sparse nodes data can provide an economic yet effective solution for automatic model building with FWI in areas of complex salt for exploration. Moreover, they also reveal that the major challenge of sparse nodes data is the reduced S/N of the FWI model due to weaker stacking power from the increased spatial sampling. Given the good balance between data quality and cost, sparse nodes acquisition is becoming a preferred solution for exploration in geologically complex regions. Following a survey design study through synthetic modeling in the WGOM region (Blanch et al., 2019), BHP acquired a sparse nodes survey in this extremely challenging area in 2018.

Sparse OBN data at WGOM

This sparse OBN survey was mainly intended for automatic velocity model building using FWI for exploration purposes. Earlier studies found that, for velocity updates with FWI, a node spacing of 1 x 1 km is an acceptable range (Mei et al., 2019) and energies at far offsets that turn back from the basement are critical for velocity updates beneath thick salt bodies (Blanch et al., 2019). This survey was acquired with a node spacing of 1 x 1 km and a relatively large shot spacing of 200 x 400 m (two local areas with 100 x 100 m shot spacing that we refer to as "imaging shots"). It has a node coverage of 2400 km^2, acquired in a single patch, and a shot coverage of 6800 km^2, as a result of a 15 km shot halo. Consequently, this survey provides decent ultra-far offset (>40 km) coverage for updating the deep subsalt model as well as the complex overburden.

Although this sparse OBN survey provides the ultra-far offsets required for deep model updates, utilizing the ultra-far offset energies is not trivial. First, we need to properly model the ultra-far offset energies coming back from the very deep basement, which requires an appropriate basement in the model (Blanch et al., 2019). Second, the main challenge of sparse nodes data, namely the noisy update in the FWI model due to the reduced stacking power, becomes more severe since the S/N of individual traces at these ultra-

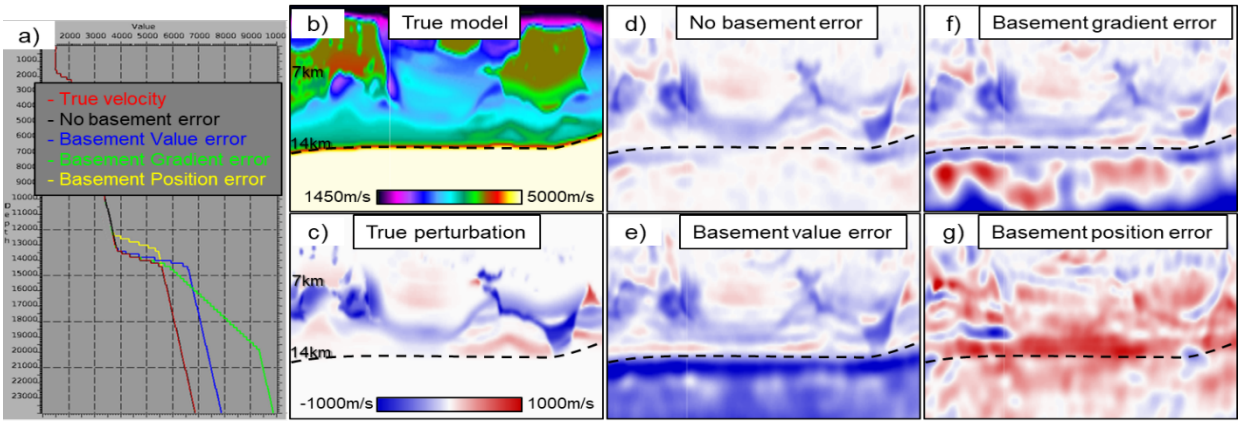

Figure 1: The impact of basement errors on FWI updates at 1.5 Hz: a) velocity profiles showing different types of basement errors introduced into the initial models for FWI; b) "True" velocity model; c) velocity errors introduced into the initial model for FWI; d) FWI updates with a perfect basement in the initial model; e)-g) FWI updates with basement errors in value, gradient, and position in the initial model, respectively.

far offsets is poorer as a result of earth attenuation and geometrical spreading of the signals. In addition, a nearby acquisition introduced strong seismic interference (SI) noise, which made the S/N issue even worse. The relatively large sparsity, especially on the source side, combined with the poor S/N of individual traces at ultra-far offsets and the strong SI noise, could introduce significant noise and large uncertainties into the derived velocity model. Therefore, properly modeling the turning wave energies from the far offsets and mitigating the noise issue are the two most critical factors for using this sparse nodes data for velocity updates.

Sparse nodes for velocity

In this area, the diving waves passing through the deep subsalt area mostly make their turns at the interface of the basement and are recorded at the ultra-far offsets (>40 km) (Blanch et al., 2019; Blanch et al., 2020). For this reason, having a basement in the velocity model is a necessary step to properly model the diving wave energies and use them for the FWI update. However, it is challenging to define both the basement position and velocity accurately due to a lack of constraints. As a result, there are potentially three types of errors related to the basement in the input model to FWI: 1.) Basement velocity value errors, 2.) Basement velocity gradient errors, 3.) Basement position errors.

We performed a set of synthetic studies to understand the impact on the inversion results from each of these three types of errors. Starting from the legacy velocity model, we built a "True" geological model with thick and complex salt bodies (Figure 1b). On top of the "True" model, we introduced some errors into the salt geometry and sediment velocity (Figure 1c) to create a base model for four FWI test scenarios: "exact basement" and three types of basement errors (Figure1a). Without any basement errors, the "True" model could be recovered well thanks to the diving wave energy recorded at far offsets (Figure1d). Among these three types of basement-related velocity errors, the "True" velocity model above the basement could be reasonably inverted with incorrect basement velocity value or gradient (Figures 1e and 1f), while the inversion failed to give correct updates when the basement position was incorrect (Figure 1g). However, a correct basement position could still be inferred from where large perturbations appear in this incorrect update. This results from the fact that the basement layer has much faster velocities, so its position errors can easily introduce large velocity errors to the initial model for FWI and cause cycle-skipping issues in FWI updates. Thus, this synthetic study demonstrates that a correct basement position is the most critical factor for utilizing the far-offset diving wave energies for FWI velocity updates.

As the legacy model still had large overburden velocity errors in this survey area, the basement was not accurately positioned in the initial model for FWI, which caused cycle-skipping. However, in contrast to the synthetic test, which was more of an extreme case with ~1 km of global basement positioning errors, the positioning errors in the real case were more local and with varying degrees. Therefore, iterative FWI and manual interpretation of the basement was carried out to gradually improve the basement positioning and converge to a better velocity model.

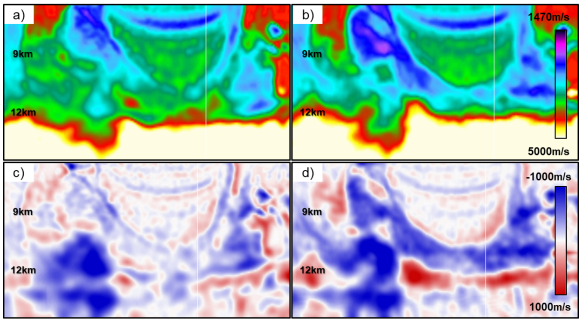

Figure 2: a)/c) velocity model and perturbation derived from TLFWI without structural and TV regularization; b)/d) velocity model and perturbation derived from TLFWI with structural and TV regularization.

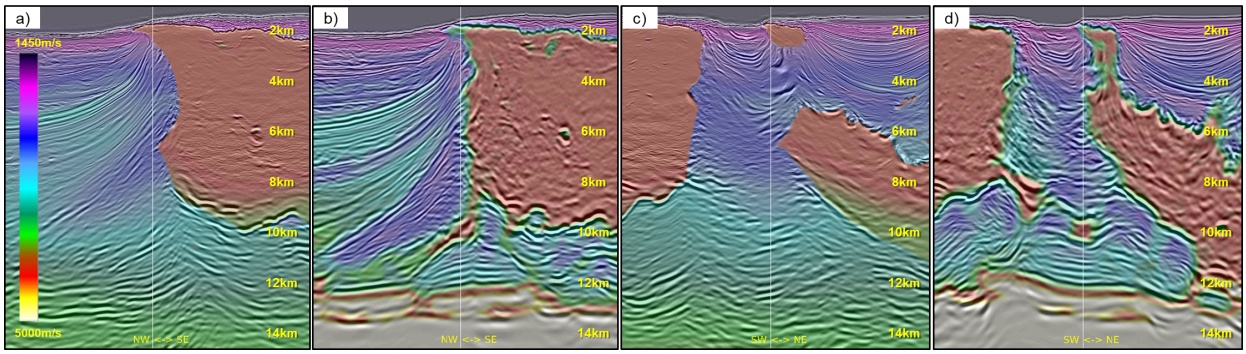

Figure 3: 15 Hz WATS RTM stack using legacy and final 8 Hz TLFWI models: a) Crossline view of the legacy velocity and stack, b) Crossline view of the final 8 Hz velocity and stack c)/d) Inline view of velocity and stack from legacy model and final model, respectively.

Besides the basement position, another major challenge is the noisy update in the FWI model due to large shot and node spacing, poor S/N of ultra-far offset data, and strong SI noise. Although Time-lag FWI (TLFWI) can handle data with low S/N better than conventional algorithms (Zhang et al., 2018), the TLFWI-updated model from this sparse nodes data is still very noisy, especially at deep sections (Figures 2a and 2c). Moreover, the strong noise in the model makes it very difficult for FWI to fully converge to a kinematically accurate and geologically plausible model. To mitigate the noisy updates in the model, we further improved the TLFWI algorithm by introducing structural and total variation (TV) regularization into the cost function (Xue el al., 2020). The improved TLFWI algorithm resulted in cleaner updates and better-defined geological features such as shale bodies. Therefore, it helped converge to a better model (Figures 2b and 2d).

With the iterative workflow to build a better basement and an improved FWI algorithm, we managed to derive a more accurate velocity model with improved geological details. Contrasted with the legacy model, this updated velocity model better delineated the complex geometry of the salt and shale bodies, and it led to a WATS RTM image with better-defined subsalt structures and improved event continuity and focusing (Figure 3).

Sparse nodes for imaging

Because of its limited offsets (<9 km) and azimuth, the existing WATS data lacks illumination and often cannot fully image some complex subsalt areas, even with a greatly improved velocity model (Figures 4a and 4d). Therefore, we went a step further and used the sparse nodes data for imaging as well. Thanks to the increased subsalt illumination from the ultra-long offsets and full-azimuth coverage of the sparse nodes data, the migration image using the fully preprocessed sparse nodes data shows improved structure and event continuity over the WATS image at various locations. However, it is noisier overall and has a lower resolution due to the lower stacking power from sparse sampling and the larger contribution from large-angle reflection energy to the image, still making it difficult to use for interpreting the subsalt structures (Figures 4b and 4e).

Recently, FWI Imaging has been shown to produce images of higher S/N and improved illumination through the use of full-wavefield data and iterative least-squares data fitting (Zhang et al., 2020; Huang et al., 2021). By using the full-

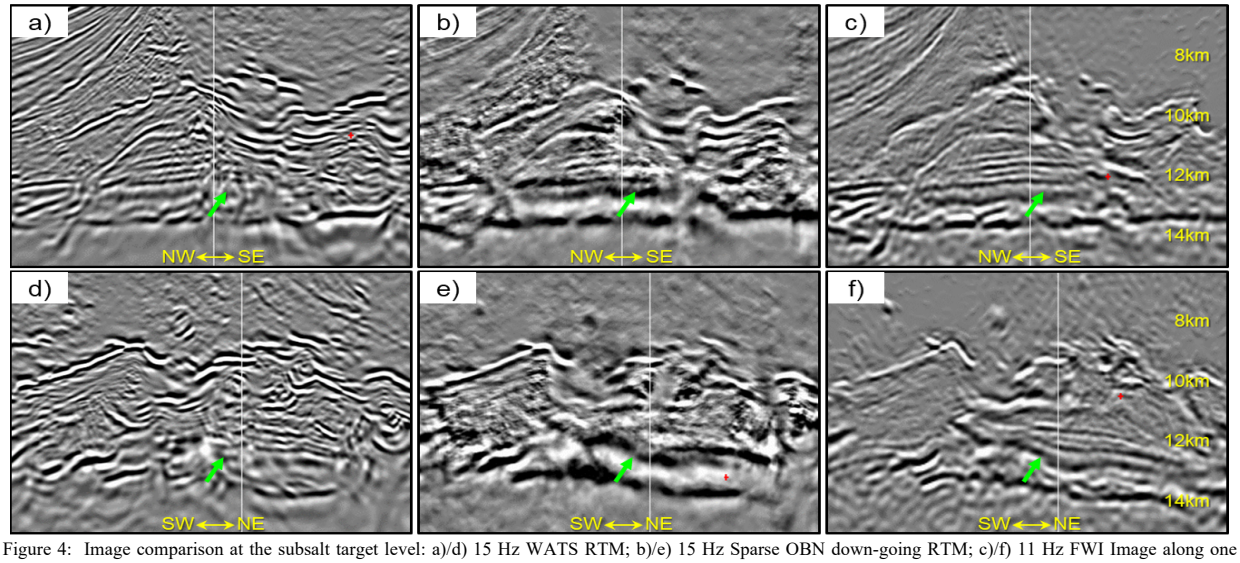

Figure 4: Image comparison at the subsalt target level: a)/d) 15 Hz WATS RTM; b)/e) 15 Hz Sparse OBN down-going RTM; c)/f) 11 Hz FWI Image along one crossline and one inline, respectively.

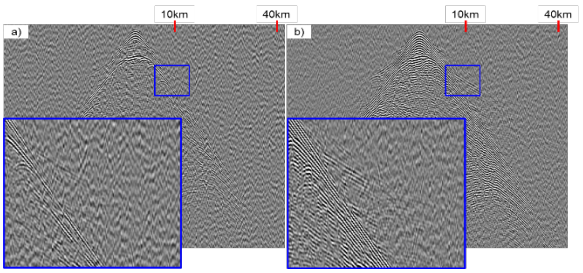

Figure 5: Data domain comparison: a) conventional airgun data below 4 Hz, b) EFS data below 4 Hz. Blue boxes show the zoomed-in areas at ~10 km offset with mostly diving wave energies.

wavefield data that includes reflection and transmission waves, primaries, and multiples, FWI Imaging of sparse nodes data produced a cleaner image and better-defined structures than either sparse OBN RTM or WATS RTM (Figures 4c and 4f). Thus, it provided a better volume for subsalt structure mapping in this area.

Low-frequency source experiment

Given that the limited S/N is the primary challenge of sparse nodes data, a seismic source emitting stronger low-frequency signals could be beneficial, at a given acquisition sparsity, for velocity model building and imaging by improving the S/N of individual traces. This results from the fact that FWI relies on the low-frequency signals to correct for the low-wavenumber velocity errors, and the low-wavenumber velocity largely determines the kinematics of the wave propagation. At the end of the WGOM sparse nodes survey, 9 source lines of Gemini Extended Frequency Source (EFS) prototype data at a spacing of 150 x 4000 m were acquired for experimental purposes. Figure 5 shows that the Gemini EFS prototype generates more low-frequency energy than a conventional air-gun array.

To confirm the benefits of EFS data, we performed a TLFWI test using this EFS data and compared the result to the ones obtained from the conventional airgun data at its original shot spacing of 200 x 400 m, as well as the decimated one at 200 x 2000 m which has a similar shot density as EFS. The fold ratio of the decimated conventional airgun data, EFS, and non-decimated conventional airgun data is 1.5:1:7.5 (Figures 6a-6c). Compared with FWI updates using the decimated conventional airgun data, shallow updates using EFS data appear to be quite similar, while deeper updates are obviously cleaner from the EFS data even though the EFS data has 1/3 less fold (Figures 6d and 6e). With more than 7 times the number of traces, the non-decimated conventional airgun data shows much cleaner top-down updates than the EFS data (Figures 6e and 6f). This control test demonstrates that, at a similar trace density, EFS can provide a cleaner FWI model because EFS can generate stronger signals at low frequencies and thus better S/N from near to far offsets. However, we still need a reasonable trace density to ensure sufficient stacking power for inverting a good velocity model, especially in geologically complex regions.

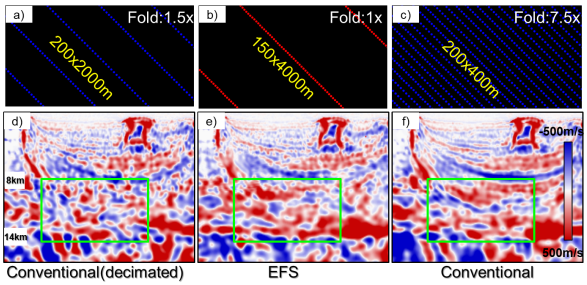

Figure 6: Shot map and TLFWI perturbation using different data: a)/d) conventional airgun with decimation, b)/e) EFS, c)/f) conventional airgun without decimation.

Conclusions and Discussions

The WGOM sparse nodes survey provided good improvements to the velocity model and images in this study area of very complex overburden and deep subsalt targets. Nonetheless, some significant challenges were met during the processing of this survey. In particular, to make use of the ultra-far offset data for FWI updates, a basement with correct positioning is needed in the initial model for FWI, as demonstrated in the synthetic study. We had to iterate FWI and manual interpretation to progressively improve the basement and the velocity model to solve this challenging problem. Additionally, an improved FWI algorithm with structural and TV regularization was helpful for mitigating the strong noise issue in this sparse nodes survey and allowing the inversion to converge to a better velocity model. Finally, FWI Imaging, which models and uses the full-wavefield data, further unlocked the potential of this sparse nodes data set and provided an improved image for subsalt structure mapping that went beyond the initial expectations of this sparse nodes survey. However, it is worth noting that some true velocity details may not be fully inverted with this sparse nodes data or could be lost during noise attenuation through regularization, eventually leading to some image degradation. This is evident in the results in that we generally see better velocity details and images in the areas closer to the imaging shots of denser sampling.

To further improve the sparse nodes survey for velocity model building and imaging, a better low-frequency seismic source and/or denser shot spacing can be used to improve the S/N of individual traces and the overall stacking power, respectively. On the algorithm side, as the larger-angle reflection or transmission energies have stronger elastic effects, moving the FWI modeling engine from acoustic to elastic could allow us to better use these energies and obtain improved results in FWI model updates and FWI Imaging.

Acknowledgments

We thank CGG, BHP, and WesternGeco for permission to publish this work.

REFERENCES

Dellinger, J., A. J., Brenders, J. R., Sandschaper, C., Regone, J., Etgen, I., Ahmed, and K. J., Lee, 2017, The Garden Banks model experience: The Leading Edge, **36**, 151–158, doi: https://doi.org/10.1190/tle36020151.1.

Huang, R., Z., Zhang, Z., Wu, Z., Wei, J., Mei, and P., Wang, 2021, Full-waveform inversion for full-wavefield imaging: Decades in the making: The Leading Edge, doi: https://doi.org/10.1190/tle40050324.1.

Mei, J., Z., Zhang, F., Lin, R., Huang, P., Wang, and C., Mifflin, 2019, Sparse nodes for velocity: Learnings from Atlantis OBN full-waveform inversion test: 89th Annual International Meeting, SEG, Expanded Abstracts, 167–171, doi: https://doi.org/10.1190/segam2019-3215208.1.

Michell, S., X., Shen, A., Brenders, J., Dellinger, I., Ahmed, and K., Fu, 2017, Automatic velocity model building with complex salt: Can computers finally do an interpreter's job?: 87th Annual International Meeting, SEG, Expanded Abstracts, 5250–5254, doi: https://doi.org/10.1190/segam2017-17778443.1.

Shen, X., I., Ahmed, A., Brenders, J., Dellinger, J., Etgen, and S., Michell, 2017, Salt model building at Atlantis with full- waveform inversion: 87th Annual International Meeting, SEG, Expanded Abstracts, 1507–1511, doi: https://doi.org/10.1190/segam2017-17738630.1.

Wang, P., Z., Zhang, J., Mei, F., Lin, and R., Huang, 2019, Full-waveform inversion for salt: A coming of age: The Leading Edge, **38**, 204–213, doi: https://doi.org/10.1190/tle38030204.1.

Xue, Z., Z., Zhang, F., Lin, J., Mei, R., Huang, and P., Wang, 2020, Full-waveform inversion for sparse OBN data: 90th Annual International Meeting, SEG, Expanded Abstracts, 686–690, doi: https://doi.org/10.1190/segam2020-3427891.1.

Zhang, Z., J., Mei, F., Lin, R., Huang, and P., Wang, 2018, Correcting for salt misinterpretation with full-waveform inversion: 88th Annual International Meeting, SEG, Expanded Abstracts, 1143–1147, doi: https://doi.org/10.1190/segam2018-2997711.1.

Zhang, Z., Z., Wu, Z., Wei, J., Mei, R., Huang, and P., Wang, 2020, FWI imaging: full-wavefield imaging through full- waveform inversion: 90th Annual International Meeting, SEG, Expanded Abstracts, 656–660, doi: https://doi.org/10.1190/segam2020-3427858.1.

Blanch, J., J., Jarvis, C., Hurren, A., Kostin, Y., Liu, and L., Hu, 2020, Designing an exploration-scale OBN: Acquisition design for subsalt imaging and velocity determination, The Leading Edge, **39**, 248–253, doi: https://doi.org/10.1190/tle39040248.1.